

ELECTRICAL CONDUCTIVITY AND OPTICAL STUDIES ON $\text{Bi}_{3.25}\text{La}_{0.75}\text{Ti}_{2.97}\text{V}_{0.03}\text{O}_{12}$ MODIFIED $70\text{Bi}_2\text{O}_3$ - $20\text{B}_2\text{O}_3$ - 10TiO_2 GLASSES

V. Venkatesh, Md. Shareefuddin and N.V. Prasad*

Materials Research Laboratory, Department of Physics, Osmania University, Hyderabad-07, India.

*Corresponding Author nvp1969@rediffmail.com

Abstract : Aurivillius ferroelectric modified bismuth boro-titanate glasses, namely $x [\text{Bi}_{3.25}\text{La}_{0.75}\text{Ti}_{2.97}\text{V}_{0.03}\text{O}_{12}] - (100-x) [70\text{Bi}_2\text{O}_3-20\text{B}_2\text{O}_3-10\text{TiO}_2]$ with $x=30, 40, 50, 60$ were prepared by melt quenching method. The XRD measurements were made on the above samples. Detailed optical spectroscopic measurements were performed on the glass matrix. Impedance, FTIR and Raman spectroscopic measurements were also performed on the above-said glass matrix. Impedance data was measured in the frequency range of 100 Hz to 1MHz to study the electrical conductivity response of BLTV on a boro-bismuth titanate glass system. Complex Impedance spectroscopic plots have shown broad spike behavior at higher frequency regions. The Raman spectroscopic plots were found to be helpful for understanding the dielectric modes of the samples. In the optical studies, the band gap energy was found to increase with increasing ferroelectric composition. From the overall studies, it is concluded that the present glass composites can be used for non-linear optical applications.

Keywords: AC-conductivity, Cole-Cole, glass-matrix, impedance spectroscopy, Raman modes, SEM pictures,

Date of Submission: 12-06-2025

Date of Acceptance: 25-06-2025

I. Introduction

Ferroelectric-based glass materials have shown excellent electrochemistry and are used for electro-optic devices [1]. The electrical properties of glass matrices depend upon the transition metal ions, especially vanadium modified glass matrix materials. Owing to the fact that multiple valance states of vanadium either V^{4+} and V^{5+} , the conduction mechanism in these materials is dominated by means of polaron hopping mechanism [2-4]. The properties of the present glasses mainly depend on the interconnectivity of structural compositional and processing parameters [2-4]. Ceramic glasses are generally divided into crystalline and amorphous materials called glass ceramic materials [2]. Some of the properties of glass ceramics make them unique so that no other material satisfies the modern technical requirements. The advantage of glass ceramics is that it combines the ease of fabrication of glass with the properties of ceramic material, such as high strength and stiffness etc. [5,6].

Mixed-bismuth oxide layer compounds of Aurivillius family, were reported by Bengt Aurivillius in 1949 and thereafter a number of compounds were investigated [7,8]. Among all the ferroelectrics, bismuth-based material is found to be a promising ferroelectric material. The properties like high curie temperature, high dielectric constant, large break down strength and excellent polarization make these materials as future promising materials [9].

Bismuth borate glasses are of great interest to researchers due to their applications in various fields. Borate glasses have high chemical durability and thermal stability [10]. Glasses based on Bi_2O_3 have a wide variety of applications in the field of optoelectronic devices, mechanical and thermal sensors, reflecting windows etc. [11]. The glasses with ferroelectric crystals embedded in them are of great demand since they exhibit unique properties. Among ferroelectrics, bismuth titanate is one of the promising perovskite ferroelectric compounds due to its non-linear electro-optic coefficient [9]. However, only a few studies have been reported on the electrical and optical properties of glass ceramics. Glass ceramics materials have low thermal expansion and high toughness. Moreover, they are very resistant to thermal shocks [6-8]. In the present investigation, we have studied the properties Bi_2O_3 - B_2O_3 - TiO_2 (BBT) glass matrix, embedded with $\text{Bi}_{3.25}\text{La}_{0.75}\text{Ti}_{2.97}\text{V}_{0.03}\text{O}_{12}$ (BLTV) ferroelectric material with different compositions, as given in the Table1. The proportions of B_2O_3 and TiO_2 are kept constant while the proportions of BBT and BLTV are varied in appropriate manner. The compositions of BBT and BLTV are shown below in the Table1.0.

In the present work, we have prepared BLTV powder embedded in the glass matrix (BBT) using a conventional melt quenching method. A detailed XRD analysis was made to understand the crystalline-glass

mixed nature. Optical and Raman spectroscopic studies were made on the samples. Detailed ac-conductivity studies were also made on the composition. Such systematic studies have not yet been reported so far.

Table 1. Composition of (100-x) BBT-x BLTV glass matrix.

S.NO	(100-x) BBT (wt%)	(x)BLTV (wt%)	SAMPLE CODE
1	40	60	BBT40+BLTV60
2	50	50	BBT50+BLTV50
3	60	40	BBT60+BLTV40
4	70	30	BBT70+BLTV30

II. Methodology

The ceramics powder samples of glasses were prepared using a melt-quenching method. Firstly, the ferroelectric compound, namely $\text{Bi}_{3.25}\text{La}_{0.75}\text{Ti}_{2.97}\text{V}_{0.03}\text{O}_{12}$ (BLTV), was prepared by adopting a solid-state reaction method using Bi_2O_3 , La_2O_3 , TiO_2 and V_2O_5 as reactant compounds. These powders were taken in the stoichiometric ratio and grounded in a planetary ball mill for 12 hours. The mixture was then calcinated at 900°C for four hours. The calcinated powder was milled again for 12 hours in the ball mill. Then we prepared glass samples by taking Bi_2O_3 , B_2O_3 and TiO_2 in the stoichiometric ratio and BLTV was added to the glass matrix in the composition as mentioned in Table 1. The mixtures were then taken in porcelain crucibles and heated for 40 min at 1200°C to obtain a molten state. The molten sample was quickly quenched by pouring onto a pre-heated stainless-steel plate and then pressed immediately with another plate. The samples which were prepared were observed as transparent glasses. The BBT-BLTV glass samples were fabricated using the composition: (100-x) BBT + x BLTV (with x = 30, 40, 50, 60 wt%).

X-ray diffraction studies of the above prepared glass ceramics were recorded using PanAnalyticX'pert plus diffractometer. The Cu-K_α (1.54\AA) radiation was used and the scanning was done at suitable scattering rate $2^\circ/\text{min}$. The densities of all prepared glass samples were measured by using Archimede's principle in xylene (density $0.87\text{gm}/\text{cm}^3$) as liquid media. Fourier Transform Infrared (FTIR) spectra of the glass ceramic samples was recorded by using FTIR -8400S Shimadzu in the wavenumber range $200\text{--}2000\text{ cm}^{-1}$. The optical measurements were done with the help of UV 3092 UV-VIS spectrometer. Impedance spectroscopic measurements of the samples were also performed, using Autolab (PGSTAT-30) impedance analyzer. Before performing the impedance measurements, the overall surfaces of the samples were coated with silver pasted and annealed in IR lamp for 1 hour. SEM images were obtained with help of ZEISSFESEM. Raman spectra were recorded in the range of $50\text{ to }2000\text{ cm}^{-1}$, using a laser wavelength of 785 nm , produced by the Horiba Jobin Yvon Raman spectrometer.

III. Results and discussions

The XRD patterns of (100-x) BBT + x BLTV (x=30,40,50,60 wt.%) glass systems were shown in Fig 1a-1d. From Fig. 1e, we can conclude the formation of BLTV by observing all the characteristic peaks related to $\text{Bi}_{3.25}\text{La}_{0.75}\text{Ti}_{2.97}\text{V}_{0.03}\text{O}_{12}$, JCPDS no. 35-0795. From the plot, it is concluded that the pure BLTV sample has shown all the characteristics of peaks related to BLTV. Some of the XRD peaks were indexed for samples BBT50-BLTV50 and BBT40-BLTV60. Low concentrations of BLTV samples, namely BBT70-BLTV30 and BBT60-BLTV40, have not shown any XRD peaks, which clearly indicates the amorphous or glass nature of the sample. On increasing BLTV composition, the amorphous phase is transformed slowly into the crystalline phase. It can be seen from Fig. 1 that BBT50+BLTV50 and BBT60-BLTV40 samples have both amorphous and crystalline phases.

Fig. 2(a-d) shows scanning electron microscope photographs of the glass-ceramic composites. From the photographs, it is evident that surface morphology is changing from an amorphous nature to a mixed amorphous and polycrystalline nature. This type of mixed nature is attributed to the growth of odd and even planes of (117) and (2 0 4) and (1 1 3) of pseudo-orthorhombic.

The density values(ρ) are measured for all the prepared glass samples which are given in Table 2. Density was calculated by using the following formula:

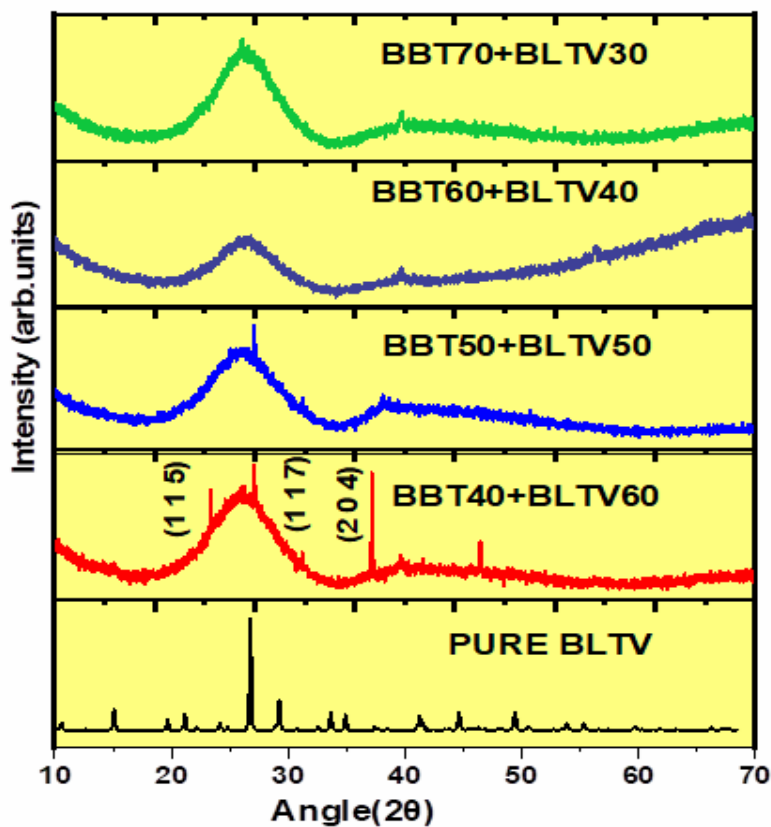


Fig 1. XRD pattern of BBT-BLTV glass-matrix samples.

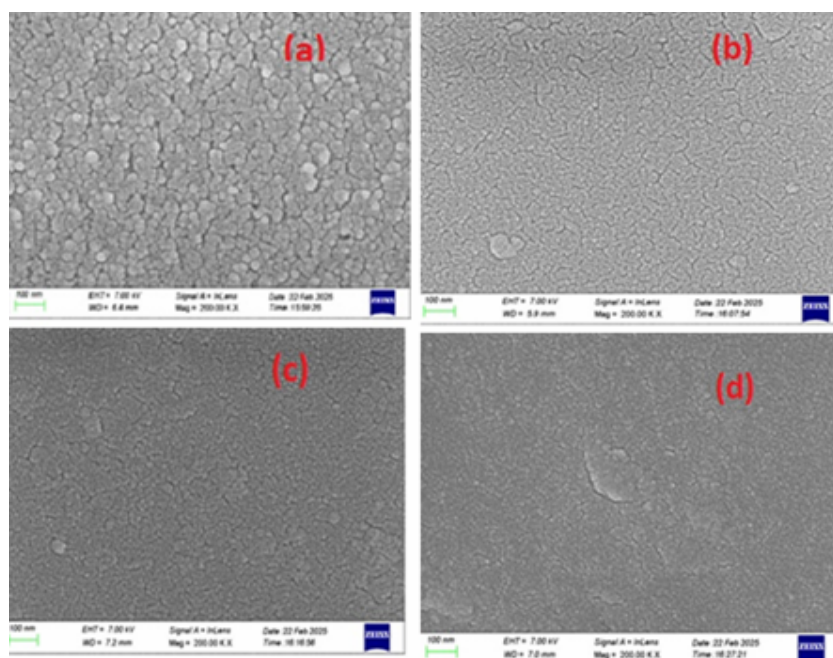


Fig 2. SEM images of all glass –matrix samples (a) BBT40+BLTV60 (b) BBT50+BLTV50 (c) BBT60+BLTV40 (d) BBT70+BLTV30.

$$\rho = \left(\frac{w_a}{w_a - w_b} \right) \times \rho_b \quad (1)$$

Where ρ_b - is the density of the reference liquid (xylene=0.865 g/cc) . The terms w_a and w_b represent the weight of the prepared glass samples measured in air and xylene respectively. Molar volume was calculated by using the formula:

$$V_m = \frac{M_c}{\rho} \quad (2)$$

Where M_c is the molecular weight of the glass-ceramic sample. In Table 2, the molar volume values were found to increase with the increase in BLTV content. Transition metal ion concentration (N) can be calculated by using the following relation:

$$N = \frac{0.01 \times N_A \times f}{V_m} \quad (3)$$

Where N_A is Avogadro number, ρ is density and V_m is molar volume of the glass sample. Transition metal ion concentration is found to decrease with an increase of BLTV content. Polaron radius of the glass matrix was calculated by using the following formula:

$$r_p = \left(\frac{1}{N} \right)^{1/3} \quad (4)$$

Polaron radius values are found to increase with the increase in BLTV content. The interionic distance of the constituent atoms can be calculated by using the formula:

$$r_i = \frac{1}{2} \left(\frac{\pi}{6N} \right)^{1/3} \quad (5)$$

The Oxygen Packing Density (OPD) can be calculated by using the following formula.

$$\text{OPD} = \frac{100 \times \rho \times O_i}{M_c} \quad (6)$$

Interionic distance values also found to increase with the increase in BLTV content. The calculated physical parameters like Density, Molar volume, Transition Metal Ion Concentration, Polaron radius, Inter Ionic distance, Optical Band Gap, and Urbach Energy of different Glass Compositions are shown in Table 2.

Table 2.0 Density, Molar volume, Transition Metal Ion Concentration, Polaron radius, Inter Ionic distance, Optical Band Gap, and Urbach Energy of $(100-x)[0.70\text{Bi}_2\text{O}_3-0.20\text{B}_2\text{O}_3-0.10\text{TiO}_2] + x [\text{Bi}_{3.25}\text{La}_{0.75}\text{Ti}_{2.97}\text{V}_{0.03}\text{O}_{12}]$, where, x=60,50,40,30 wt%.

SL. NO	Sample	Density (gm/cc)	Molar Volume (cc/mol)	Transition Metal ion concentration (Ni)1020/cc	Polaron radius (\AA)	Interionic distance (\AA)	Oxygen Packing Density (OPD)	E_{opt} (eV)	Urbach energy (eV)
1	BBT40+ BLTV60	6.25	120.12	3.13×10^{20}	1.47×10^{-7}	5.93×10^{-8}	166.50	2.59	0.16
2	BBT50+ BLTV50	6.22	110.20	3.39×10^{20}	1.43×10^{-7}	5.78×10^{-8}	181.48	2.61	0.13
3	BBT60+ BLTV40	6.19	100.18	3.72×10^{20}	1.39×10^{-7}	5.61×10^{-8}	199.64	2.64	0.12
4	BBT70+ BLTV30	6.56	84.57	4.67×10^{20}	1.29×10^{-7}	5.19×10^{-8}	236.49	2.66	0.10

The optical absorption of the glass ceramic composites of the composition $(100-x) (0.70\text{Bi}_2\text{O}_3-0.20\text{B}_2\text{O}_3-0.10\text{TiO}_2) + x$ BLTV was recorded at room temperature in the wavelength range 200-1000 nm. The UV-Visible spectra of glass samples were shown in Fig. 3a. From Fig. 3 it is observed that a decrease in the concentration of Bi_2O_3 . The absorption edges were found to shift towards the lower wavelength side. Fig. 3c shows the Davis and Mott plots of all the glass samples. The optical band gap values were calculated, and the values are given in Table 2.0. From this it is evident that as the concentration of BBT increases, the optical band gap also increases. This difference in the optical band gap values is mainly due to the formation of non-bridging oxygen linkages. From these results it was observed that optical band gap values varied with the composition of glass samples. The absorption coefficient(α) was calculated by using the following formula:

$$\alpha = \frac{1}{d} \log\left(\frac{I_0}{I}\right) \quad (6)$$

Where d represents the thickness of the sample, I_0 and I represent the intensity of the incident and transmitted light beam respectively. The absorption coefficient (α) and optical band gap (E_g) are related by the equation:

$$\alpha h\nu = [B(h\nu - E_g)]^r \quad (7)$$

The constant B is independent of energy (E) which is known as the band tailing parameter and $h\nu$ is the photon energy. Index r is a constant that determines the type of optical transition. The constant r can have different values, like $1/3$, $1/2$, 2 , 3 . These values would correspond to direct forbidden, direct allowed, indirect allowed, and indirect forbidden respectively. In the present case, the value of constant r is $1/2$ which corresponds to the direct band gap transition. The values were found to be consistent with our earlier results on similar compounds [12].

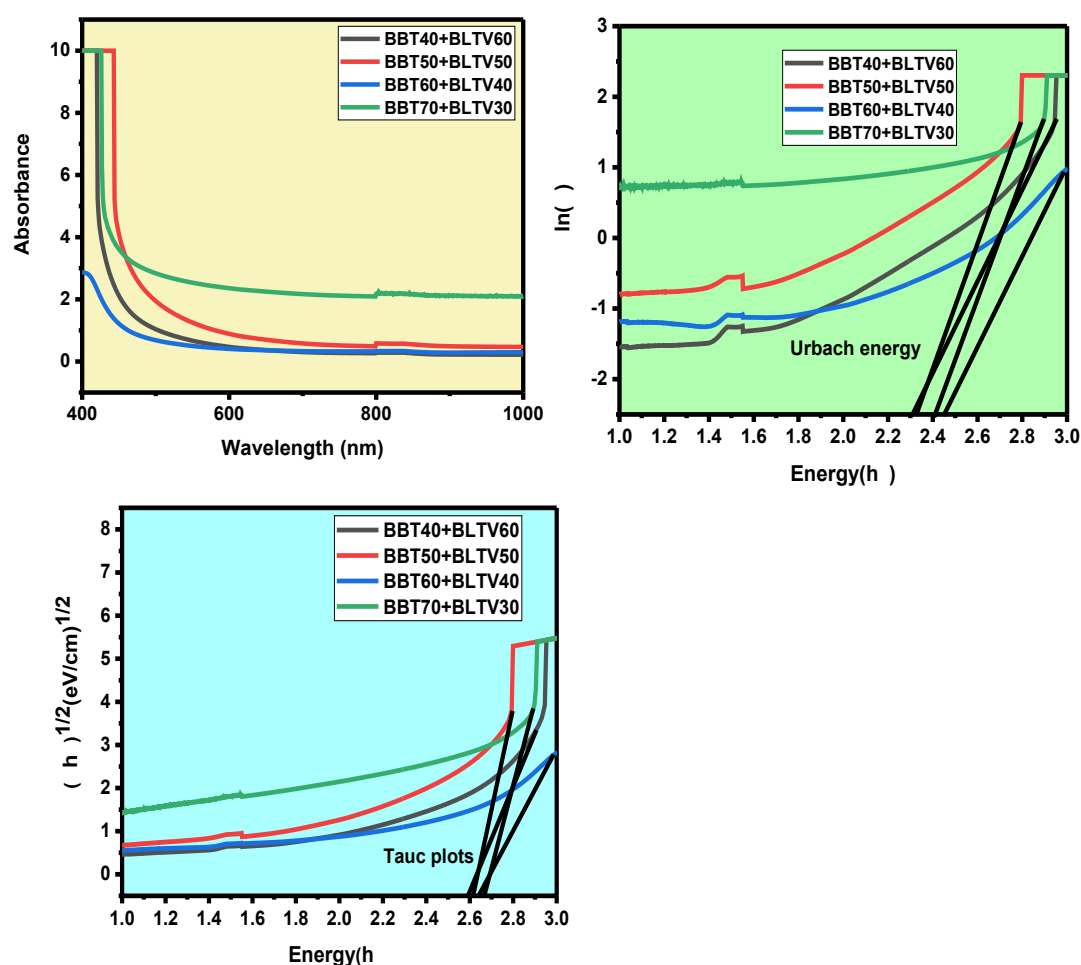


Fig 3. (a) Optical absorption spectra of all glass matrix samples. (b) Urbach energy of glass matrix compositions. (c) Tauc's plots of glass matrix samples.

The graph drawn between $h\nu$ and $(\alpha h\nu)^r$ is known as Tauc's plot (Fig. 2c), from which one can calculate the optical band gap energies of the samples. E_g values were obtained by extrapolating the linear region of the curves to meet $h\nu$ axis i.e. where $(\alpha h\nu)^r = 0$. The calculated values of E_g were listed in Table 2. Urbach energy is a measure of the disorderly nature of the system. If the Urbach energy is high, then the materials have a better tendency to convert weak bonds into defects [12]. From the plots of log of absorption coefficient vs photon energy, Urbach energies of all glass samples were calculated. The slopes of the straight lines obtained from plotting $\log(\alpha)$ vs $h\nu$, were first calculated.

The reciprocals of these values give the Urbach energies, which are depicted in Table 1. The small range of energy values suggests the presence of minimal defects in the present glass system. From the table, it is also observed that Urbach energy decreases as the glassy nature increases. This is due to the structural disorder observed in the glass system and the combined effect of glass-ceramic nature [13].

To extract more about dielectric nature of the samples, the following well known Urbach equation is used:

$$\alpha(\nu) = \alpha_0 \exp\left(\frac{h\nu}{\Delta E}\right) \quad (8)$$

Urbach energy represents input photon energy. $\alpha(\nu)$ is the absorption coefficient. The E_{opt} values were found to increase with decreasing the BLVT composition. An increase in E_{opt} can be attributed to bismuth-borate interaction. Boron network contains more B3O units, compared to B4O units. Therefore, the increasing E_{opt} can be ascribed to decreasing the trend of non-bridging oxygen (NBO) network. Here it cannot be ruled out that the competitive interaction of both non-bridging and bridging oxygens also exists. However, non-bridging oxygen's magnitude increases with the borate network. Moreover, non-bridging oxygens are flexible and energetic to respond the rigid bridging oxygen vacancies. The decreasing Urbach energy is responsible for increasing the order nature of the sample. The results were consistent with E_{opt} values [13]. Small values of Urbach energy suggest an inclination towards order nature, which explains the local order. Such a local order explains the dielectric nature of the present glass ceramic matrix. The relation between the refractive index and the dielectric constant is given by:

$$\frac{(n^2-1)}{(n^2+2)} = 1 - \sqrt{\frac{E_g}{20}} \quad \text{and} \quad \epsilon = n^2 \quad (9)$$

Here 'n' represents refractive index and ' ϵ ' is dielectric constant. Molar refractivity (R_m) of the materials explains the total polarization based on the mole of the substance. The relation for R_m is:

$$\text{Molar refractivity } (R_m) = \frac{(n^2-1)}{(n^2+2)} \times V_m \quad (11)$$

The term ' V_m ' represents molar volume. The electronic polarization can be obtained by the product of charge and displacement of the electron cloud in the presence of electron cloud. Metallization criterion explains the characteristics of metallization or non-metallization process. Electronic Polarizability (α_m) and Metallization criterion (M) relations are given below:

$$\text{Electronic Polarizability } (\alpha_m) = \frac{3}{4\pi N_A} \times R_m \quad (12)$$

$$\text{Metallization criterion } (M) = \left(1 - \frac{R_m}{V_m}\right) \quad (13)$$

The above-mentioned values n, R_m , α_m , ϵ and M are shown in the Table 3.0.

Table 3. Refractive index(n), Dielectric constant(ϵ), Molar refractivity (R_m), Electronic Polarizability(α_m) and Metallization criterion(M) values for all the compositions.

Sample code	Refractive index (n)	Dielectric constant (ϵ)	Molar refractivity (R_m)(m ³ /mol)	Electronic Polarizability (α_m)(C.m ² .V ⁻¹)	Metallization criterion (M)
BBT40+BLT60	2.517	6.33	76.893	3.0493×10^{-23}	0.3598
BBT50+BLT50	2.510	6.30	70.390	2.7914×10^{-23}	0.3612
BBT60+BLT40	2.501	6.25	63.782	2.5294×10^{-23}	0.3633
BBT70+BLT30	2.495	6.22	53.728	2.1306×10^{-23}	0.3646

The Fourier Transform Infrared Spectroscopy of the present glass composition was recorded at room temperature in the range of $400\text{--}2400\text{ cm}^{-1}$ which is shown in Fig. 4. The significant absorption band observed at 448 cm^{-1} is assigned to the vibrations of metal cations (Ba^{2+} , VO^{2+}). The peak corresponding to $510\text{--}530\text{ cm}^{-1}$ in all the glass samples may be assigned to the Bi-O bending vibrations of BiO_6 octahedral units [14]. The small peak present at 547 cm^{-1} is assigned to the stretching mode of an oxygen atom between three vanadium atoms or V-O bond. The peak, which appears at 627 cm^{-1} corresponds to Bi-O stretching vibration mode. The peak attributed to 715 cm^{-1} signifies the B-O-B linkage network. The peak appearing at 788 cm^{-1} indicates Ti-O-Ti symmetric vibrations of TiO_4 . The peak appearing at 1047 cm^{-1} signifies B-O stretching vibrations of tetragonal $[\text{BO}_4]$ units in tri, tetra and Penta borate groups. The peak corresponding to 1242 cm^{-1} is assigned to tetrahedral BO_4 units, connected to titanium ions. The peak attributed near 1400 cm^{-1} shows asymmetric vibration modes of non-bridging oxygen of the B-O-B matrix. The peak corresponding to 1527 cm^{-1} signifies asymmetric stretching vibrations of BO_3 units in meta-borate, pyro-borate and ortho-borate groups. From the above graph, it is concluded that BLTV composition in the glass matrix influences the structure of glass and acts as a network modifier.

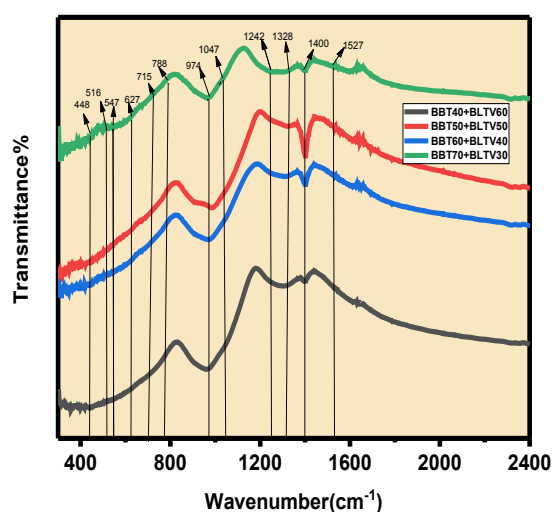


Fig 4. FTIR spectra of prepared glass matrix.

Raman studies were made on glass composites at room temperature. The Raman shift is observed from $100\text{--}4000\text{ cm}^{-1}$. Raman spectra obtained for all the composite samples is shown in Fig. 5, along with their deconvoluted spectra. The peak which appeared at 106 cm^{-1} is due to symmetric stretching vibrations of Bi-O and its linkages. The peaks at 151 cm^{-1} and 161 cm^{-1} signify the vibrational modes which are related to displacement of oxygen ions corresponding to bismuth vibrations due to highly polarizing heavy metal Bi^{+3} ions associated with $[\text{BiO}_3]$ pyramidal and $[\text{BiO}_6]$ octahedral units. From this it is clear that the role of bismuth is glass former in the network.

The peak, which appears at 890 cm^{-1} , is attributed to Ti^{+4} ions associated with 4-, 5- and 6-fold coordinate units such as $[\text{TiO}_4]$, $[\text{TiO}_5]$ and $[\text{TiO}_6]$. A peak observed at 1049 cm^{-1} is assigned to non-bridging oxygen (NBOs) of [Bi-O] associated to $[\text{BiO}_3]$ units. The peak at 1236 cm^{-1} signifies bending vibrations of the $-\text{OH}$ group of water molecules. The peaks arising in the range 2400 cm^{-1} is mainly due to free and weakly H-bonded hydroxyl molecules.

Complex impedance spectroscopic data extracted from the impedance data were obtained in the range of $100\text{ Hz--}1\text{ MHz}$ at different temperatures (Room temperature- 2500C). The variation of the imaginary part of impedance (Z'') with the real part of impedance for all the prepared glass-ceramics samples is shown in Fig. 6. From the plots, it is evident that with increasing BLVT composition, the spike nature is found to tune gradually to a semicircular nature. These results were consistent with our earlier results [12]. This type of partially incomplete semicircle is ascribed to the disordered nature of the glass-matrix. This type of dielectric relaxation is generally called non-Debye relaxation or multiple behavior. As the concentration of BLTV increases in the glass matrix, the dispersion in the data decreases due to the bulk nature of the glass ceramic sample.

The vertical spike nature for low concentration of BLTV indicates the double layer capacitance of the sample. From this one can conclude that an equivalent RC circuit can be constructed by the combination of bulk resistance and constant phase element (CPE) start playing role in the conduction process. This type of behavior is generally observed in all glasses. The variation of ac-conductivity with frequency at different temperatures is shown in Fig.6(a-d). From the conductivity data, more dispersion was observed in the low frequency region for low concentration of BLTV. In addition, two distinct regions were clearly observed for low concentrations of BLTV as compared to the higher concentration of sample (BBT40-BLVT60).

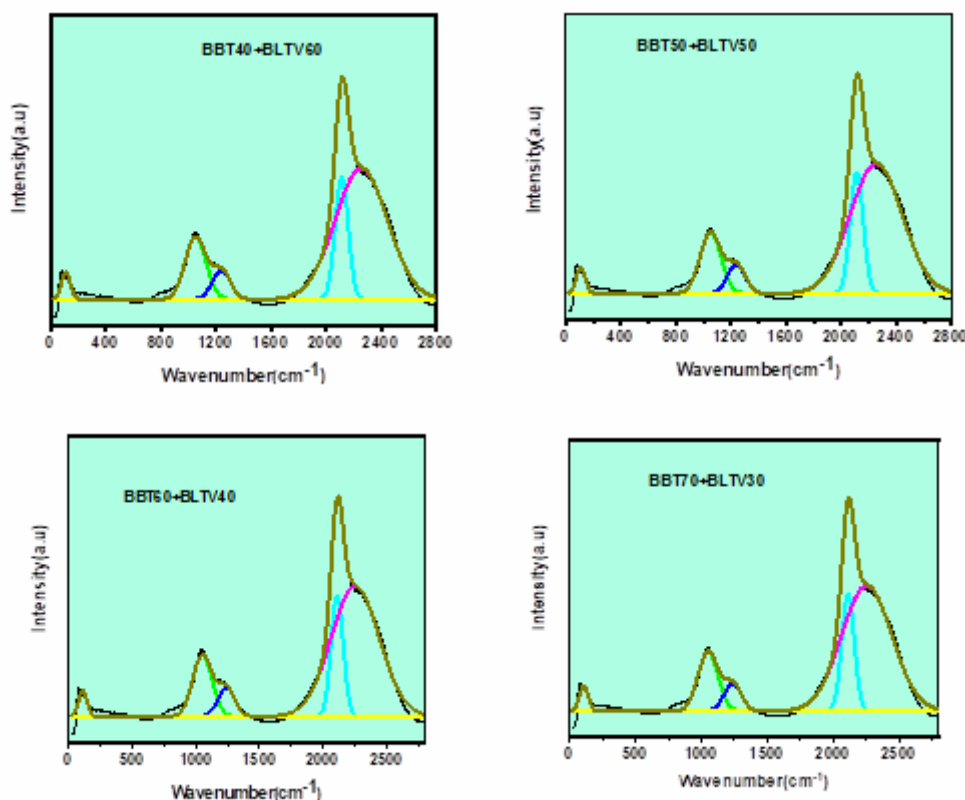


Fig 5. Raman spectra and its deconvolution of all prepared glass composites.

The variation of ac-conductivity with frequency obtained at different temperatures is shown in Fig. 6. From the fig, it is evident that three distinct regions, namely n_1 , n_2 and n_3 , are observed. The three distinct regions suggest the thermally activated conduction phenomenon of the samples. In region one, the conduction is found to be frequency independent. This suggests the random ionic diffusion process via a hopping mechanism. An increase in the conductivity values with the increasing temperature is attributed to the thermally activated process. The energy of the charge carriers is also found to increase with frequency. The degree of interaction between the lattice and mobile ions can be understood in the overlapping region n_2 . The same can be confirmed due to the hopping between multi-states of vanadium ion, as pointed out earlier. The normalized conductivity data obtained at different frequencies for all the samples is shown in Fig. 6. The overlapping of data into a single curve indicates that the conduction mechanism is independent of temperature. In other words, the dynamic process that takes place at different frequencies has the same thermal activation energy. Addition of BLTV in the glass-matrix leads to the reduction of the metallization criterion. Based on the metallization values, one can conclude that these materials may have future nonlinear optical applications [13,14].

The variation of ac-conductivity with frequency obtained at different temperatures is shown in Fig. 7. From the fig, it is evident that three distinct regions, namely n_1 , n_2 and n_3 are observed. The three distinct regions suggest the thermally activated conduction phenomenon of the samples. In region one, the conduction is found to be frequency independent. This suggests the random ionic diffusion process via a hopping mechanism. An increase in the conductivity values with the increasing temperature is attributed to the thermally activated process. The energy of the charge carriers is also found to increase with frequency. The degree of interaction between the lattice and mobile ions can be understood in the overlapping region n_2 . The same can be confirmed due to the hopping between multi-states of vanadium ion, as pointed out earlier. The normalized conductivity data obtained

at different frequencies for all the samples is shown in Fig. 7. The overlapping of data into a single curve indicates that the conduction mechanism is independent of temperature. In other words, the dynamic process takes place at different frequencies and has the same thermal activation energy. Addition of BLVT in the glass-matrix leads to the reduction of the metallization criterion. Based on the metallization values, one can conclude that these materials may have future nonlinear optical applications [13-15].

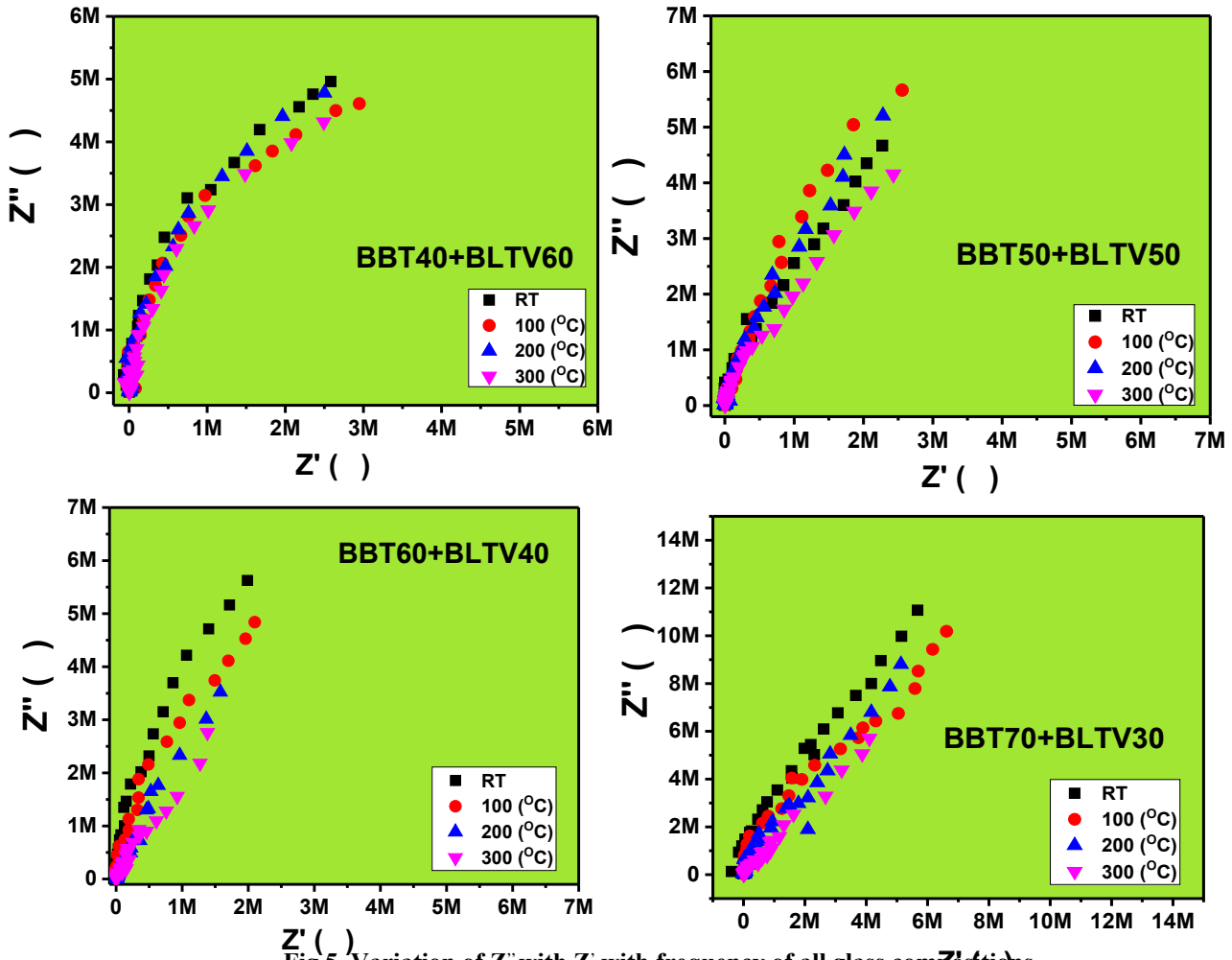


Fig 5. Variation of Z'' with Z' with frequency of all glass compositions

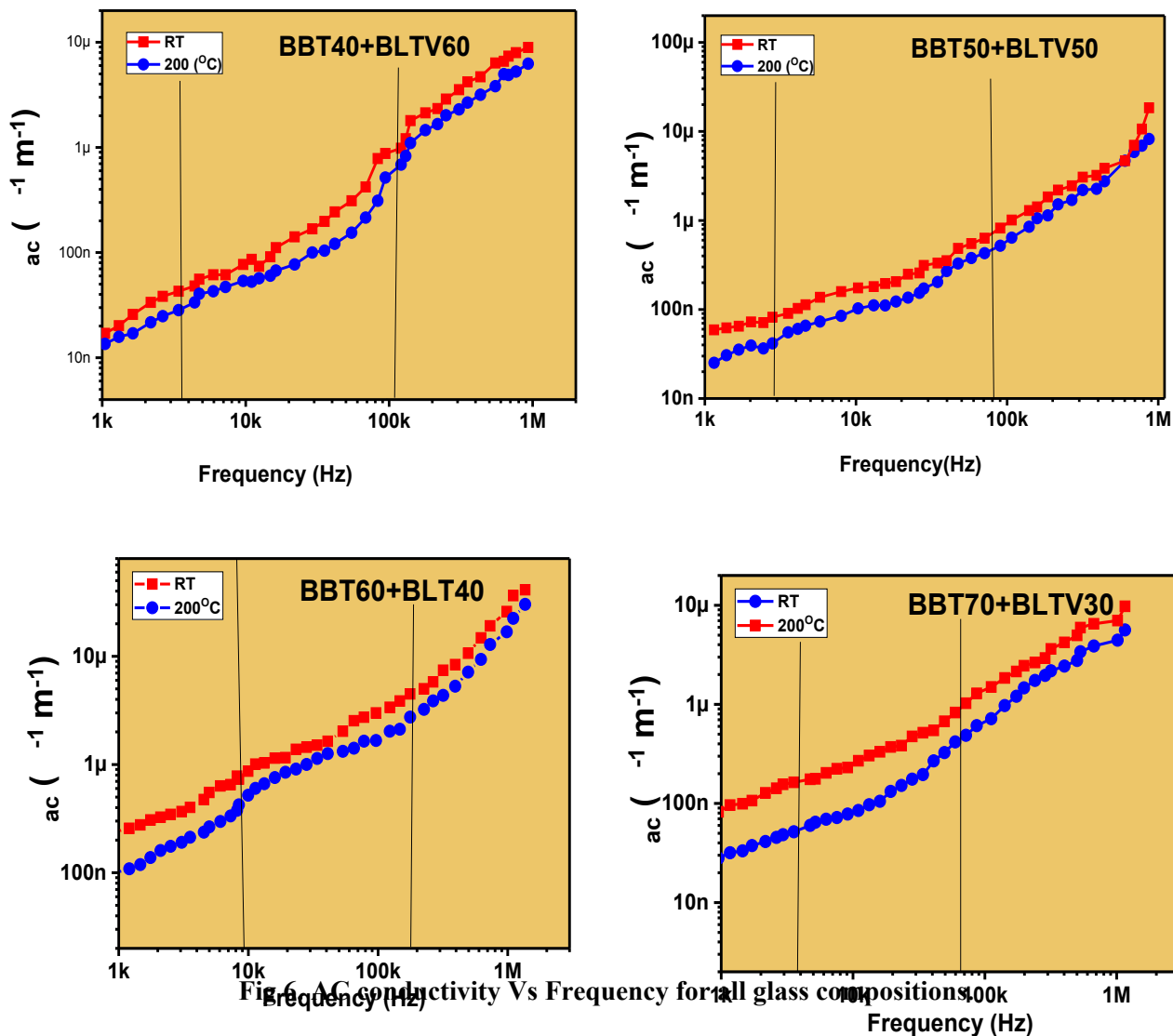


Fig. 6. AC conductivity Vs Frequency for all glass compositions

IV. Conclusions

Based on the overall electrical and Raman spectroscopic studies, the dielectric properties were attributed to the overall collective nature of the dipoles. The dielectric polarization results were to be consistent with the Raman data. Detailed ac-conductivity data show two slope regions. This indicates the frequency-dependent and frequency-independent nature. From this, it is concluded that the overall conductivity is due to hopping between charge clusters and thermal migration of the ions. Moreover, the relaxation species were found to be temperature-independent. The spectroscopic peaks are found to appear in the same frequency region, which explains the same. Based on the earlier results on similar compounds, it is concluded that the present glass matrix samples belong to nonlinear optic-materials and can be used in optical-switching, optical-computing, optical-data storage etc.

Acknowledgements

One of the authors, V. Venkatesh is thankful to the ACE Engineering College, Hyderabad for supporting the research work.

References

- [1]. Wolfram, H., George, B.: Glass-ceramic technology, American Ceramic Society, Ohio, (2002).
- [2]. K. Majhi, K.B.R. Varma, Dielectric relaxation in $\text{CaO-Bi}_2\text{O}_3\text{-B}_2\text{O}_3$ glasses, *Int. J. Appl. Ceram. Technol*, 7 (2010) 89-97.
- [3]. S. Sailaja, C. Nageswara Raju, C.A. Reddy, B.D.P. Raju, Y.D. Jho, Optical properties of Sm^{3+} doped cadmium bismuth borate glasses, *J. Mol. Struct.* 1038 (2013) 29-34.
- [4]. E.K. Abdel-Khalek, I.O. Ali, Structural, ac conductivity and dielectric properties of vanado-tellurite glasses containing BaTiO_3 , *J. Non Cryst. Solids* 390 (2014) 31-36.
- [5]. A. Ghosh, S. Bhattacharya, A. Ghosh, Optical and other physical properties of semiconducting cadmium vanadate glasses, *J. Appl. Phys.* 101 (2007) 083511.
- [6]. CR Gautam, Abhishek Madheshiya, "Fabrication methods of lead titanate glass ceramics and dielectric characteristics: a review", *J. Mat. Sci.: Mat. in Elect.*, 31, (2020) 12004.
- [7]. Harizanova R, Slavov S, Vladislavova L, Costa LC, Avdeev G, Bocker C, et al. "Barium titanate containing glass-ceramics - The effect of phase composition and microstructure on dielectric properties". *Ceram. Int.*, 46, (2020) 24591.
- [8]. Thakur S, Vanita Thakur, Kaur A, Singh L. "Study of the Crystallization and structural behavior of bismuth barium titanate Glass-Ceramics". *J. non-Crys. Solids.*, 557, (2021) 120563.
- [9]. Ramana EV, Prasad NV, Tobaldi DM, Zavašnik J, Singh MK, Hortigüela MJ, et al. "Effect of samarium and vanadium co-doping on structure, ferroelectric and photocatalytic properties of bismuth titanate". *RSC Advances.*, 7, (2017) 9692.
- [10]. P. Pascuta, G. Borodi, E. Culea, Structural investigation of bismuth borate glass ceramics containing gadolinium ions by X-ray diffraction and FTIR spectroscopy, *Mater. Sci. Mater. Electron.* 20 (2009) 360-365.
- [11]. Zhao Z, Liang X, Zhang T, Hu K, Li S, Zhang Y. "Effects of cerium doping on dielectric properties and defect mechanism of barium strontium titanate glass-ceramics". *J. Euro. Ceram Soc.*, 40, (2020) 719.
- [12]. V. Venkatesh, D. Sreenivasu, B. Ravinder Reddy, Md. Shareefuddin, G. Ramadevudu and N.V. Prasad, Electrical and Optical Studies on Lanthanum Bismuth Titanate Modified Boro-Bismuth Titanate Glass-Matrix. *ECS J. Solid State Sci. Technol.* 14 (2025) 04301113.
- [13]. F. El-Diasty, F.A.A. Wahab, Optical band gap studies on lithium aluminum silicate glasses doped with Cr^{3+} ions, *J. Appl. Phys.* 100 (2006) 093511.
- [14]. Ahmed MR, Sekhar KC, Hammed A, Chary MN, Shareefuddin M. Role of aluminum on the physical and spectroscopic properties of chromium-doped strontium alumino borate glasses. *Int. J. Modern Physics B.* 32 (2018) 1850095–1850095.
- [15]. Sayed MA, Ali AM, El-Rehim AFA, Wahab EAA, Shaaban KS. Dispersion Parameters, Polarizability, and Basicity of Lithium Phosphate Glasses. *J. Electronic Materials.* 50 (2021) 3116–3128.